

# RSC Advances



This is an *Accepted Manuscript*, which has been through the Royal Society of Chemistry peer review process and has been accepted for publication.

*Accepted Manuscripts* are published online shortly after acceptance, before technical editing, formatting and proof reading. Using this free service, authors can make their results available to the community, in citable form, before we publish the edited article. This *Accepted Manuscript* will be replaced by the edited, formatted and paginated article as soon as this is available.

You can find more information about *Accepted Manuscripts* in the [Information for Authors](#).

Please note that technical editing may introduce minor changes to the text and/or graphics, which may alter content. The journal's standard [Terms & Conditions](#) and the [Ethical guidelines](#) still apply. In no event shall the Royal Society of Chemistry be held responsible for any errors or omissions in this *Accepted Manuscript* or any consequences arising from the use of any information it contains.

Cite this: DOI: 10.1039/c0xx00000x

www.rsc.org/xxxxxx

ARTICLE TYPE

# Fast switching of liquid crystals on transferred reactive mesogens film via soft imprinting method

Hong-Gyu Park, Hak Moo Lee, Hae-Chang Jeong, and Dae-Shik Seo<sup>a,\*</sup>

Received (in XXX, XXX) Xth XXXXXXXXX 20XX, Accepted Xth XXXXXXXXX 20XX

DOI: 10.1039/b000000x

Unidirectional alignment of liquid crystal (LC) molecules is a prerequisite for advanced LC devices. We present a novel approach for the alignment of LC molecules. The process consists of reactive mesogen (RM) stamp production, RM transfer onto a polyimide (PI) layer, and LC device fabrication. Physicochemical and optical measurements show that thin films of RMs are well transferred onto PI layers from the RM stamp via contact printing. Uniform and unidirectional alignment of the LC molecules is achieved on the RM/PI surfaces. In addition, the pretilt angles of the LC molecules can be controlled by the compositions of the bottom PI layers. The no-bias-bend  $\pi$ -cell using RM/blended PI polymeric stacks exhibits superior electro-optical properties.

## Introduction

Liquid crystal displays (LCDs) are used extensively in various applications because they are thin and portable and consume little power. Achieving sophisticated control and uniform alignment of liquid crystal (LC) molecules with a regular pretilt angle on a polyimide (PI) layer is an important step in the manufacture of LCDs<sup>1,2</sup>. The function of the LCD relies on the proper treatment of the confining surfaces for precise orientation of the LC molecules. Mechanical rubbing has been widely used to provide topographical microgrooves that enable the uniaxial homogeneous or homeotropic alignment of LCs<sup>3</sup>. However, the rubbing process has several disadvantages, including the generation of dust, electrostatic charges, and mechanical stress, all of which can be detrimental to LCD applications<sup>4</sup>. Therefore, a non-contact alignment technique would be better suited for the task. Alternative methods for aligning the layers include photo-alignment<sup>5,6</sup>, self-assembled monolayers<sup>7</sup>, and ion-beam irradiation<sup>8-10</sup>. Although these noncontact approaches are free from electrostatic charge and dust generation, they suffer from alignment instability, low anchoring energy, and image sticking<sup>11</sup>. In addition, many researchers have employed specific surface topographies to uniformly align the LC molecules using various methods such as laser writing<sup>12</sup>, electron-beam writing<sup>13</sup>, microrubbing<sup>14</sup>, dip-pen lithography<sup>15</sup>, rigiflex lithography<sup>16</sup>, and soft lithography<sup>17</sup>. Although these methods allow more freedom to control the alignment properties such as the pretilt angle, anchoring energy, and multistability compared to conventional methods, the performance of the resultant LC devices built on such a series of surface-patterned alignment layers is inferior to that of LCDs containing PI alignment layers<sup>18-19</sup>. Moreover, most of the patterned LC alignment layers exhibit weak optical properties because the surface pattern induces light loss due to the scattering of light by the surface grating<sup>20-23</sup>. Therefore, there is a

need to develop a novel fabrication method for advanced LC alignment that can solve all of the above problems.

Here, we demonstrate the use of reactive mesogen (RM) transfer onto conventional PIs from a UV-cured RM stamp treated by a rubbing process via contact printing to induce stable LC ordering. The reusable RM stamp was fabricated by UV exposure and rubbing to obtain optically anisotropic properties. When detached from the stamps, the resulting RM films can be used to successfully align the LC molecules in one direction. In addition, the pretilt angles of the LC molecules can be controlled according to the conditions of the bottom PI layers. We can achieve a no-bias-bend (NBB)  $\pi$ -cell with no initial bias voltage and a fast response time (RT) by combining the RMs and blended PIs. Our LC devices exhibit superior electro-optical (EO) properties.

## Experiment

To fabricate the RM stamps, RM (RMS03-015, Merck) monomers were coated onto a glass substrate via spin coating (3000 rpm for 30 sec). These films were cured using a nonpolarized ultraviolet (UV) exposure system (Oriel Co.) to obtain a uniform UV energy density of 80% of its original UV energy. Light from a high pressure mercury lamp (Nanotek Co. 1kW) was passed through an IR filter (59341, Oriel Co.) and a broad bandpass filter ( $\lambda=310-330$  nm) to isolate a specific wavelength range of light. The incident angle and exposure time for UV irradiation were 90° and 15 min, respectively. To induce anisotropy, the surfaces of the RM stamps were rubbed using a rubbing machine (NMS-RB, Namil motion system). The rubbing strength was optimized and set at 300 mm. The blended PIs (JSR Co. Ltd., Japan) used for the homogeneous and homeotropic alignment layers were prepared at various concentration. These PIs were deposited uniformly onto indium tin oxide (ITO)-deposited glass substrates by spin-coating. The blended PIs were then pre-baked on a hot plate at 80°C for 10 min and imidized in

an oven at 230°C for 1 h. The resulting films were approximately 50 nm thick. After these processes, we pressed the prepared RM stamps onto the PI/ITO target substrate for 10 min and then peeled them away. The resultant substrates were fabricated in an antiparallel configuration, and the NBB  $\pi$ -cells were created with cell gaps of 60 and 4.25  $\mu\text{m}$  for the measurement of the pretilt angle and EO, respectively. The LCs were injected into each cell via capillary injection at room temperature. The surface morphologies of the RM-transferred PIs were analyzed using atomic force microscopy (AFM; XE-Bio, Park Systems). To confirm the optical anisotropy and the compositional transformations of the RM-transferred PIs, we measured the optical retardation (REMS-100, Sesim) and employed X-ray photoelectron spectroscopy (XPS; VG Microtech ESCA2000), respectively. LC alignment conditions were observed using a polarization microscope (BXP 51, Olympus). The EO measurements of the V-T characteristics and RT were confirmed using an LCD evaluation system (LCMS-200).

## Results and discussions

Figure 1 depicts the procedures for preparing the RM stamp and fabricating LC cells with RM-transferred PI layers. Liquid crystalline RM stamps of an anisotropic nature were fabricated in a UV system to ensure photo-polymerization of the spin-coated RM monomers on a glass substrate. The RM stamps were then rubbed to induce directional anisotropy. The base PI materials were prepared with various concentrations of homogeneous and homeotropic PI. The PI layers were spin-coated onto indium tin

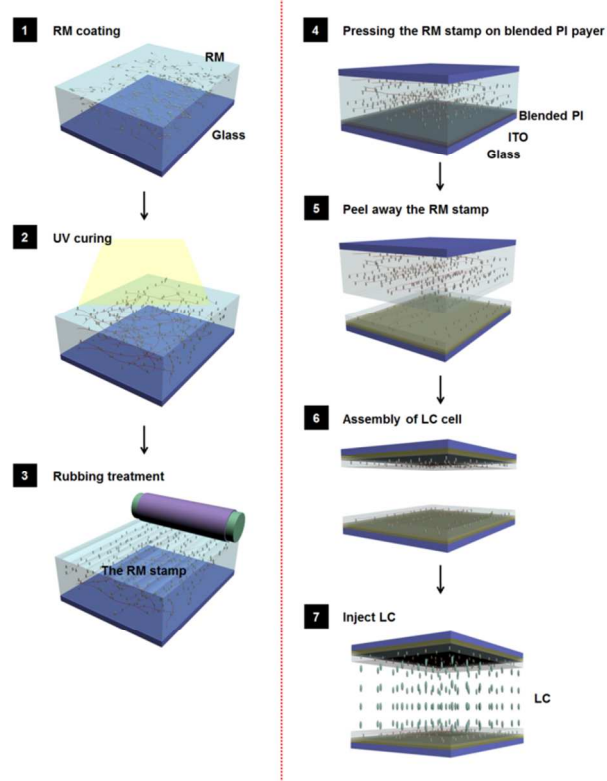


**Fig. 1** Schematic representation of the RM imprinting process. Thin films of the RMs were transferred from the RM stamps to the PI base layers to fabricate the high-performance NBB  $\pi$ -cell.

oxide (ITO)-deposited glass target substrates, which were subsequently soft and then hard baked. To transfer the RM thin films from the RM stamps to the base PI substrates, the RM stamps were placed in contact with the PI-coated ITO substrates for 10 min at room temperature and then peeled away. Using this contact imprinting method, a 10-nm-thick RM layer was printed onto the target PIs for LC alignment. Finally, positive and negative LCs were injected into sandwiched LC cells using the RM transferred PI layers to prepare the NBB-LCDs.

To verify the RM transfer to the PI surfaces, we conducted surface analysis using AFM, XPS, and optical retardation. Figure 2a shows the topographies of the RM and PI surfaces before and after rubbing treatment, as well as after RM transfer. Images were acquired in tapping mode with a  $5 \times 5 \mu\text{m}$  scan size for films with different conditions. Nonpolarized UV-cured RM and pristine PI surfaces are shown in the upper and lower left-hand corners of Figure 2a. When the RM films were rubbed by the rubbing machine, the surface roughness increased significantly. Additionally, RM transfer to the PI surfaces was confirmed based on the isomorphic shape of the RM stamps. The RMS roughness of the RM transfer surface was dramatically altered from 8.990 nm to 17.843 nm after transferring the RM thin films to the target PI surfaces.

Figure 2b shows the optical retardations of the RM stamps and the target substrates before and after the rubbing treatment, as well as after the RM transfer. The optical anisotropy of the alignment layer verified the RM transfer. Almost no retardations were observed for the nonpolarized UV-cured RM stamp and the pristine PI substrates. The nonpolarized UV irradiation only affected the RM curing without producing an anisotropic effect. The rubbing treatment induced anisotropy of the RM stamp, as shown in Figure 2b. The anisotropic property of the RM stamp was transferred by imprinting, thus changing the optical retardation of the target PI substrate. The resulting RM thin film on the target PI substrate exhibited significant optical retardation and anisotropy, indicating that the RM layer was successfully transferred from the RM stamp to the target PI substrate.

We also conducted a compositional investigation of the RM transfer onto the PI surfaces using XPS analysis to compare the XPS spectra of the PI substrates before and after imprinting to conform that the RM thin films were transferred from the RM stamps to the target PI substrates via contact imprinting. The core-level XPS spectra for the C 1s were decomposed into three components, as shown in Figure 2c. The low-binding-energy component peak centered at 284.6 eV is due to the C-C bond, whereas the peak at 286.2 eV is related to the C-O bond<sup>24,25</sup>. Another component peak at 288.5 eV corresponds to the C=O double bond in the RM stamp<sup>26</sup>. While the intensity of the C-C single bond increased significantly, the intensity of the C=O double bond decreased. The XPS spectra for the O 1s are provided for additional detail. The component peak centered at 531.6 eV corresponds to the O=C double bond<sup>27</sup>, whereas the 80 peak at 533.0 eV is due to the O-C single bond<sup>28</sup>. The intensity of the O 1s peak changed significantly due to transfer of the RM layer<sup>29,30</sup>, indicating that the intensity variations of the XPS spectra were attributable to the transfer of the RM thin film onto the PI substrate through contact imprinting.

We applied RM transfer to LC devices to examine the possibility

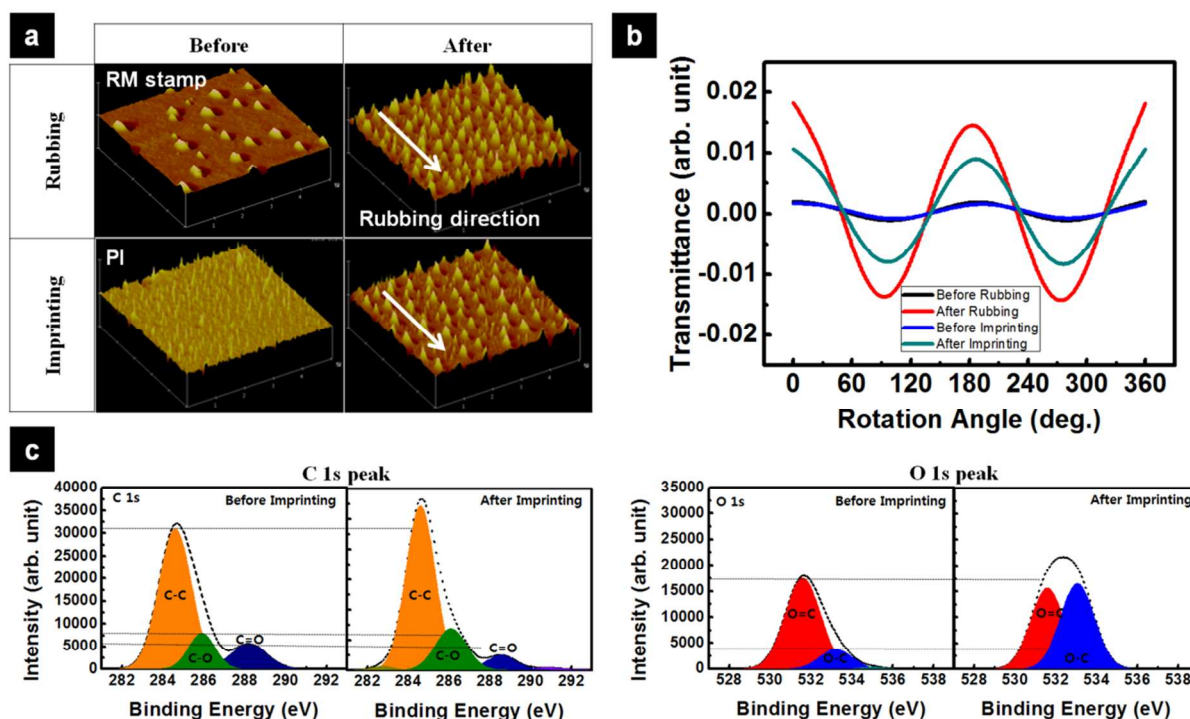


**Fig. 2** The trace of the RM transfer from the RM stamp to the base PI layers. a) AFM images for the RM stamp and the RM transfer before and after rubbing and imprinting. b) Optical retardations of the RM stamp and the target substrate before and after rubbing treatment. c) XPS spectra for C 1s and O 1s peaks confirm the RM transfer onto the PI films by contact imprinting.

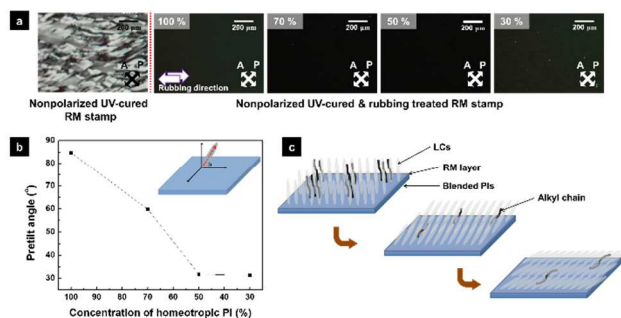


**Fig. 3** a) POM images of anti-parallel cells with the RM layers transferred from the nonpolarized UV-cured RM stamps, along with images of the UV-cured RM stamps after the rubbing treatment as a function of the concentration of homeotropic PI. b) The pretilt angle of the LC molecules on the RM/blended PIs films as a function of the concentration of homeotropic PI. c) Illustration of the mechanism underlying the changes in the pretilt angle of the LC molecules on the RM/blended PI surfaces.

of using them as a substitute for conventional PIs. To investigate the alignment states of the LCs on the transferred RM surfaces, we used polarized optical microscopy (POM), as shown in Figure 3a. From the POM images, we observed locally aligned LCs on the surface of the RM layers transferred from the nonpolarized UV-cured RM stamps. The increased anisotropy of the transferred RM layer due to the rubbing treatment of the RM stamps induced perfect LC alignment, as did conventional rubbed PIs. In addition, uniform LC alignment was achieved regardless of the concentration of blended PI under the transferred RM layer. This result indicated the potential to control the pretilt angle through the components of the lower layers. Figure 3b shows the pretilt angles of the LCs on the RM layer/blended PI layer as a

function of the concentration of homeotropic PI. The graph shows that a wide range of pretilt angles was generated by varying the concentration of homeotropic PI from 30% to 100%. The measured pretilt angles were reproducible and reliable within the error range. This result indicates that a NBB  $\pi$ -cell can be produced based on the mid-range of the pretilt angle<sup>31</sup>.

the LC molecules on the blended PIs after imprinting using the RM stamp. The mechanism of LC alignment for the RM transfer onto the blended PIs can be explained in two steps. The first is related to the change in pretilt angle of the LC molecules. The homeotropic PI alkyl side chains can produce a vertical LC alignment due to the steric repulsion between the LC molecules and the long alkyl side chain of the PIs<sup>32</sup>. Therefore, blended PIs have different side chains as a function of the concentration of homeotropic PI. As the homeotropic PI content decreases, the amount of alkyl side chains on the blended PI layer decreases. Thus, an intermediate pretilt angle is produced due to competition between the dipole-dipole/ $\pi$ - $\pi$  interactions between LC molecules and the PI backbone and steric repulsion between the LCs and the remaining alkyl side chains. When the homogeneous PI content is above 50 wt.%, the dipole-dipole and  $\pi$ - $\pi$  interaction between the LC molecules and the PI backbone are dominant, producing low pretilt angles for the LC molecules. The second mechanism involves the unidirectional and uniform LC orientation on the RM transfer caused by the rubbing-induced anisotropy. Ultra-thin RM films contribute to uniform LC alignment without affecting the underlying blended PI layers, which control the pretilt angle. In other words, the control over the pretilt angle is attributed to the combination of the RM transfer and blended PI layers. We fabricated a NBB  $\pi$ -cell with an intermediate pretilt angle of

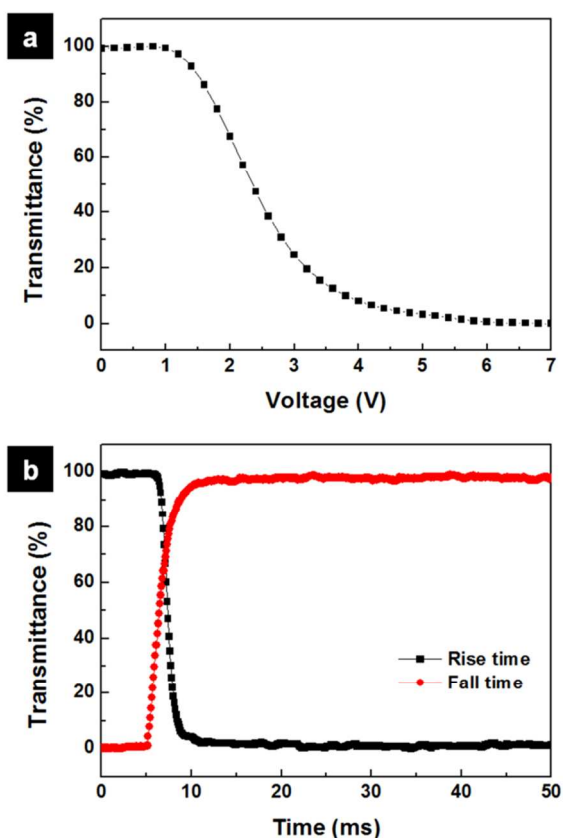


Fig. 4 a) The V-T and b) RT characteristics of the NBB  $\pi$ -cell with the RM/blended PI layers at an intermediate pretilt angle of  $59.8^\circ$ .

$59.8^\circ$  using the imprinted RMs on the blended PI layers as alignment films to examine the EO characteristics. Superior EO characteristics, including a rapid response time, were achieved in the NBB  $\pi$ -cell based on the imprinted RMs, as shown in Figure 4. The voltage-transmittance (V-T) characteristics are shown in Figure 4a. While conventional  $\pi$ -cells require an initial voltage of 1 V to create an initial bend state, the proposed layers with an intermediate pretilt angle produce a NBB  $\pi$ -cell. The pretilt angle of the NBB  $\pi$ -cell is larger than the critical angle of approximately  $48^\circ$ , which indicates that the bend state is energetically more stable than the splay state<sup>33</sup>. Therefore, the proposed NBB  $\pi$ -cell can overcome the energy barrier and maintain an initially stable bend state. At 90% transmittance, the threshold voltage of NBB  $\pi$ -cell was 1.49V. The response time (RT) characteristics, i.e., the rise time and fall time, of the NBB  $\pi$ -cell are shown in Figure 4b. The rise time was 1.8 ms, and the fall time was 3.4 ms. The total RT of 5.4 ms is 25% faster than NBB  $\pi$ -cell based on conventional rubbing-treated blended PIs<sup>34</sup>, which indicates that the combination layer of the imprinted RMs and blended PIs can potentially be used in high-performance LCD application in industrial fields.

## Conclusions

In conclusion, we demonstrated high performance VA-LCDs with RM-transferred PI alignment layers that were constructed using contact imprinting. The fabrication of an RM stamp with polarized UV curing and its successful transfer onto a base PI

were important because they resulted in both perfect alignment of the LCs and superior EO characteristics. Moreover, the VA-LC cells with our RM-imprinted alignment layers exhibited no optical loss and high thermal stability up to  $210^\circ\text{C}$ , even without capacitance hysteresis. We also elucidated the optical and compositional changes in the RM transfer process to target the PI surfaces by employing optical retardation measurement and XPS analysis, which could lead to increased precision in fabrication and the application of RM stamps for advanced flexible LCDs. We believe that by changing the combinations of RMs, base PIs and LCs, high-performance and various-mode LCDs such as twisted nematic (TN), in-plane switching (IPS), and optically compensated bend (OCB) mode LCDs can be practically fabricated.

## Notes and references

Department of Electrical and Electronic Engineering, Yonsei University, 50 Yonsei-ro, Seodaemun-gu, Seoul 120-749, Korea.. Fax: +82-2-2123-3147; Tel: +82-2-2123-4617; E-mail: [dsseo@yonsei.ac.kr](mailto:dsseo@yonsei.ac.kr)

1. M. Jiao, Z. Ge, Q. Song, and S.-T. Wu, *Appl. Phys. Lett.*, 2008, **92**, 061102.
2. S.-Y. Lu and L.-C. Chien, *Opt. Express*, 2008, **16**, 12777.
3. M. F. Toney, T. P. Russell, J. A. Logan, H. Kikuchi, J. M. Sands and S. K. Kumar, *Nature*, 1995, **374**, 709.
4. J. v. Haaren, *Nature*, 2001, **411**, 29.
5. K. Ichimura, *Chem. Rev.*, 2000, **100**, 1847.
6. M. O'Neill and S. M. Kelly, *J. Phys. D: Appl. Phys.*, 2000, **33**, R67.
7. P. Prompinit, A. S. Achalkumar, J. P. Bramble, R. J. Bushby, C. Walti, S. D. Evans, *ACS Appl. Mater. Inter.*, 2010, **2**, 3686.
8. P. Chaudhari, J. Lacey, J. Doyle, E. Galligan, S. A. Lien, A. Callegari, G. Hougham, N. D. Lang, P. S. Andry, R. John, K. Yang, M. Lu, C. Cai, J. Speidell, S. Purushothaman, J. Ritsko, M. Samant, J. Stohr, Y. Nakagawa, Y. Katoh, Y. Saitoh, K. Sakai, H. Satoh, S. Odahara, H. Nakano, J. Nakagaki, Y. Shiota, *Nature*, 2001, **411**, 56.
9. J. Stohr, M. G. Samant, J. Luning, A. C. Callegari, P. Chaudhari, J. P. Doyle, J. A. Lacey, S. A. Lien, S. Purushothaman, J. L. Speidell, *Science*, 2001, **292**, 2299.
10. Y.-G. Kang, H.-J. Kim, H.-G. Park, B.-Y. Kim, and D.-S. Seo, *J. Mater. Chem.*, 2012, **22**, 15969.
11. V. Chigrinov, A. Muravski, H. Kwok, H. Takada, H. Akiyama, H. Takatsu, *Phys. Rev. E*, 2003, **68**, 061702.
12. C. J. Newsome, M. O'Neill, R. J. Farley, G. P. Bryan-Brown, *Appl. Phys. Lett.*, 1998, **72**, 2078.
13. T. Kagajyo, K. Fujibayashi, T. Shimamura, H. Okada, H. Onnagawa, *Jpn. J. Appl. Phys.*, 2005, **44**, 578.
14. S. Varghese, G. P. Crawford, C. W. M. Bastiaansen, D. K. G. de Boer, D. J. Broer, *Appl. Phys. Lett.*, 2004, **85**, 230.
15. M. Ruetschi, P. Grutter, J. Funfschilling, H. -I. Guntherodt, *Science*, 1994, **265**, 512.
16. D. Suh, S.-J. Choi, H. H. Lee, *Adv. Mater.*, 2005, **17**, 1554.
17. S. -R. Kim, A. I. Teixeira, P. F. Neale, A. E. Wendt, N. L. Abbott, *Adv. Mater.*, 2002, **14**, 1468.
18. H.-G. Park, J.-J. Lee, K.-Y. Dong, B.-Y. Oh, Y.-H. Kim, H.-Y. Jeong, B.-K. Ju, D.-S. Seo, *Soft Matter*, 2011, **7**, 5610.
19. W.-K. Lee, Y. S. Choi, Y.-G. Kang, J. Sung, D.-S. Seo, C. Park, *Adv. Funct. Mater.*, 2011, **21**, 3843.
20. D.-R. Chiou, L.-J. Chen, *Langmuir*, 2006, **22**, 9403.
21. E. S. Lee, P. Vetter, T. Miyashita, T. Uchida, M. Kano, M. Abe, K. Sugawara, *Jpn. J. Appl. Phys.*, 1993, **32**, 1436.
22. C.-H. Chiu, H.-L. Kuo, P.-C. Chen, C.-H. Wen, Y.-C. Liu, H.-M. P. Chen, *Appl. Phys. Lett.*, 2006, **88**, 073509.
23. D.-R. Chiou, K.-Y. Yeh, L.-J. Chen, *Appl. Phys. Lett.*, 2006, **88**, 133123.
24. A. Hamwi, C. Latouche, J. Dupuis, R. Benoit, V. Marchand, *Journal Phys. Chem. Solids*, 1996, **57**, 991.

25. F. Beguin, I. Rashkov, N. Manolova, R. Benoit, R. Erre, S. Delpeux, *Eur. Polym. J.*, 1998, **34**, 905.
26. A. D. Romaschin, L. N. Bui, M. Thompson, N. B. McKeown, P. G. Kalman *Analyst*, 1993, **118**, 463.
- 5 27. C.S. K. Singamsetty, C.U. Pittman, G.L. Booth, Guo, R. He, JR. S.D. Gardner, *Carbon*, 1995, **33**, 587.
28. CH. Cardinaud, G. Lemperiere, M.C. Peignon, P.Y. Jouan, *Applied Surface Science*, 1993, **68**, 595.
29. S. G. Kim, S. M. Kim, Y. S. Kim, H. K. Lee, S. H. Lee, J.-J. Lyu, K.  
10 H. Kim, R. Lu, S.-T. Wu, *J. Phys. D: Appl. Phys.*, 2008, **41**, 055401.
30. Y.-K. K. Y.-J. Lee, S. I. Jo, K.-S. Bae, J.-H. Kim. B.-D Choi, C.-J. Yu, *Opt. Express*, 2009, **17**, 23417.
31. H.-G. Park, B.-Y. Oh, Y.-H. Kim, B.-Y. Kim, J.-M. Han, J.-Y. Hwang, and D.-S. Seo, *Electrochem. Solid-State Lett.*, 2009, **12**, J37.
- 15 32. K.-W. Lee, S.-H. Paek, A. Lien, C. Durning, H. Fukuro, *Macromolecules*, 1996, **29**, 8894.
33. J. B. Kim, K. C. Kim, H. J. Ahn, B. H. Hwang, J. T. Kim, S. J. Jo, C. S. Kim, H. K. Baik, C. J. Choi, M. K. Jo, Y. S. Kim, J. S. Park, and D. Kang, *App. Phys. Lett.*, 2007, **91**, 023507.
- 20 34. D.-H. Kim, H.-G. Park, Y.-H. Kim, B.-Y. Kim, C.-H. Ok, J.-Y. Hwang, J.-M. Han, Y.-P. Park, and D.-S. Seo, *Mol. Cryst. Liq. Cryst.*, 2010, **529**, 102.